AN EXPERIMENT TO MEASURE THE TISSUE-EQUIVALENT ABSORBED DOSE (LET) AND DEPTH-DOSE DISTRIBUTIONS PRODUCED BY RADIATIONS IN SPACE

M. C. CHAPMAN*
Northrop Space Laboratories, Hawthorne, California, U.S.A.

and

F. E. HOLLY
Air Force Weapons Laboratory, Albuquerque, New Mexico, U.S.A.

Abstract—An experiment to measure the absorbed dose distribution and depth-dose distribution in tissue-equivalent material is described. The experiment uses cellular-sized spheres of plastic scintillator to detect the dose deposition, and a pulse-height analysis is performed on the signals.

The sensor consists of a number of 100 micron spheres of plastic scintillator bonded to a lucite light-pipe. The lucite is cemented to a photomultiplier tube, and the output signal is processed by digital pulse height analyzers. This technique has many advantages over present ion chamber systems, including:

(1) measurements of absorbed dose with a detector approaching the cellular level,
(2) negligible dose gradient through the detector and minimum perturbation of the tissue-equivalent sample, and
(3) excellent resolution and gain stability.

It appears feasible to measure the absorbed dose distribution spectrum from 0.4 keV/micron to > 300 keV/micron with a single sensor. By utilizing multiple sensors with varying amounts of tissue-equivalent pre-filtering, a depth-dose distribution can be obtained. By integrating the absorbed dose spectrum, a measure of the total absorbed dose is obtained. In addition, the experiment provides data on cell hit frequency.

The removal of particle type-dependent response and geometrical considerations are discussed. One specific application of this technique involving an astronaut-manipulated space experiment is described.

INTRODUCTION

It has been well established that radiation poses a hazard to manned space flight, either through early acute effects or longer somatic effects. It is essential that dosimetric parameters such as the spectrum of radiation energy deposition and total absorbed dose be measured for small regions of tissue samples. In addition, the radiation depth-dose distribution would be important data. The experiment described in this paper utilizes very small ($\leq$ 100 micron) plastic scintillators as tissue-equivalent dosimeters, and yields measurements of absorbed dose distribution, total absorbed dose, depth-dose distribution, and cell hit frequency data not possible with present space dosimeters. The concept is based on unique application of state-of-the-art techniques of scintillation spectroscopy, and obtains data which is radiobiologically more meaningful than present "LET" devices. The dosimeter has a wide dynamic range, and can

* Now at TRW Systems Laboratories, Bedondo Beach, California, U.S.A.

perform satisfactorily in a variety of space radiation environments and missions. It is believed that this program represents a very significant scientific contribution to the knowledge of radiobiological hazards to manned space flight.

The experiment is particularly suited for missions operating within the radiation zones. The experiment will perform satisfactorily for low altitude (typically 200 n. mi.) missions or lunar flights. While it is desirable to utilize astronaut capability to modify the instrument in space, the experiment is not seriously compromised if utilized on an unmanned mission.

SCIENTIFIC BACKGROUND

The problems involved in investigating radiation hazards to living organisms in space are very complex. However, specification of the "LET" or absorbed dose spectrum, total absorbed dose, and depth-dose distribution will enable many meaningful conclusions to be drawn, using laboratory radiobiological results. No rigorous attempt will be made in this paper to scientifically justify the measurement of absorbed dose distributions or the other parameters yielded by the technique under discussion; instead, a brief summary of "LET" importance is presented.

Experiments have clearly established that the biological effectiveness of radiation depends not only on the amount of energy absorbed but also on spatial distribution of the energy deposition. Since the energy is deposited in or near the tracks of charged particles, it has been convenient to express this energy deposition in terms of the linear density of energy transfer along these tracks, or linear energy transfer. The linear energy transfer (LET) is defined as the linear rate of loss of energy ("locally absorbed") by an ionizing particle traversing a material medium. While this quantity is expressed in kiloelectron volts per micron (keV/μ), it is more rigorously a function of energy deposited per unit volume surrounding a track. The stopping power or ionization loss is a similar quantity which is defined as the loss of energy per unit path length by an ionizing particle traversing a material medium. LET emphasizes the process of energy transfer, while the stopping power emphasizes the energy lost by the particle. In the case of stopping power all energy losses resulting in the production of secondary charged particles are commonly included, while in the case of LET such losses are included only if they are absorbed in some arbitrary vicinity of the primary charged particle track.

On the basis of the physics of the energy transfer processes, estimates of LET can be made. Thus the quality of radiation can be expressed by specifying the fraction of the dose deposited in each LET interval. The LET has some utility for characterizing the ionizing track and this parameter has been found in general to correlate well with the biological effectiveness of the radiation.

While theoretically it is possible to calculate a LET distribution spectrum in a given material exposed to some specified radiation field, such calculations are quite laborious and require detailed knowledge of the flux and energy spectra of the primary radiation, and particularly the secondary particles and the material distribution around the sample. For much of the radiation encountered in space, detailed calculations are not possible since many high energy interaction cross sections are not well known. These uncertainties introduce serious errors in estimating radiation hazards since some secondaries are very heavily ionizing and generate high LET tracks.

In an environment such as a space vehicle cabin, it is currently very difficult to predict the local radiation spectra with sufficient accuracy for manned space missions. Uncertainties in the primary radiation fields, the complicated distribution of secondary particles and scattered radiation and material heterogeneity indicate that experimental determinations of LET spectra are desirable. The effect of the dose delivered in space can be approximated in the laboratory by using a combination of laboratory radiation sources to deliver a LET spectrum simulating that measured in the spacecraft.

The radiation encountered in space due to trapped radiation (VAB), solar flares (SCR), and galactic cosmic rays (GCR) will consist mainly of electrons, protons, photons, and heavier nuclei. For trapped radiation very near the earth, the electrons will produce the greatest dose for lightly shielded tissue. As shielding

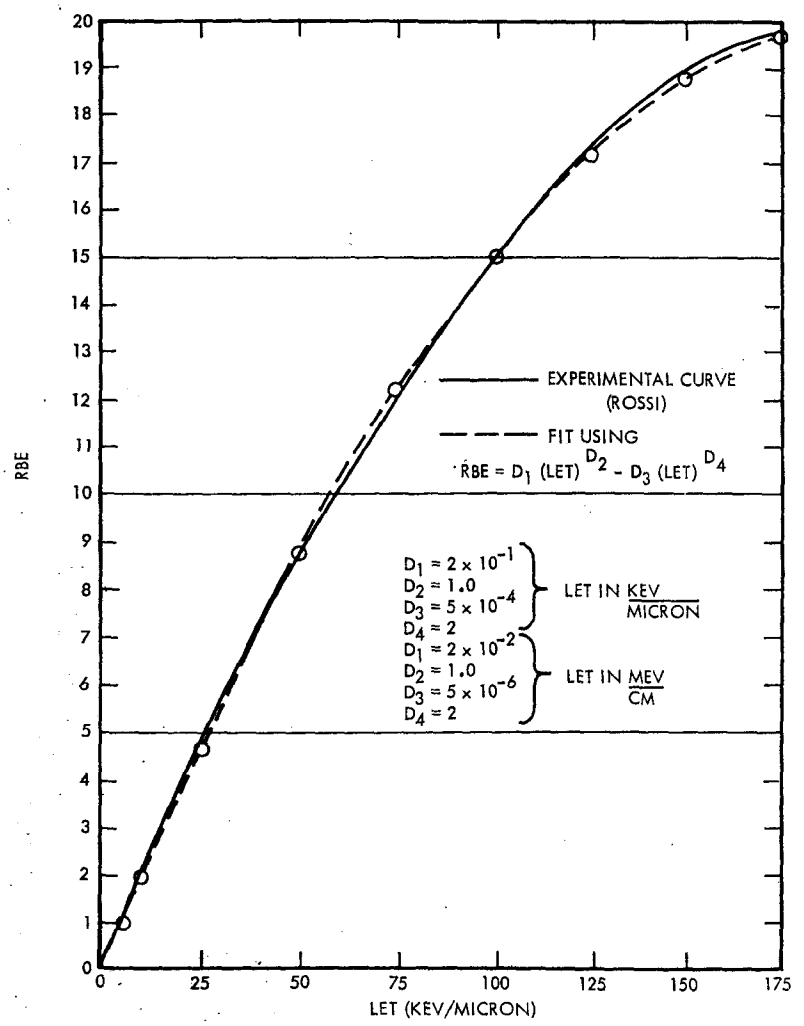

FIG. 1. RBE–LET relationship of Rossi.

increases, the proton and photon components become important. When the protons have been stopped, the photon component remains with a neutron component. Consider first the case where electrons and protons are important. Due to the steep energy spectra observed in the radiation zones, the dose gradient due to electrons and protons will be quite steep through a tissue sample. This gradient is also very important when solar flare radiation is present, since the alpha particle component is quickly attenuated in the first tissue layers.

Schaefer[1] points out that the fraction of high LET events to total dose of the alpha component of solar flares is substantially larger than the fraction of proton-induced high LET events to dose to tissue depths in excess of 10 g/cm^2. The alpha dose is especially important at small thicknesses of less than 2 g/cm^2. Schaefer recommends separate determinations of the high LET alpha and lower LET proton doses, and points out that insufficient data exists on incident spectra to permit calculation of the alpha doses under small thicknesses.

Thus, radiobiologically, it is important to determine the LET or absorbed dose distribution

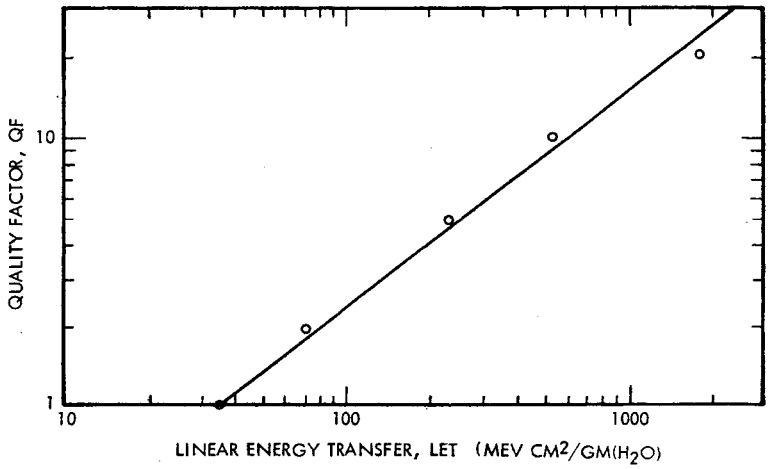

FIG. 2. The monoenergetic quality factor versus the linear energy transfer.

for both low values of LET and for high values of LET.

The importance of LET to description of radiobiological effects has been known for some time. The relative biological effectiveness (RBE) and radiation quality factor (QF)[2] both depend upon knowledge of the LET spectrum. Rossi has obtained a reasonably satisfactory relation for the dependence of RBE on LET as shown by Fig. 1[3] (after Haffner, 1964). The quality factor, LET, and dose relationship have been discussed by Madey and Stephenson,[4] where they present the LET/QF relationship shown in Fig. 2 and Table 1. The usefulness of RBE and QF is that they consider the effectiveness of the radiations in producing a biological effect for a total absorbed dose. For some biological effects, an absorbed dose (in rads) of alpha particles may be many times more damaging than the same rad dose of photons. The ratio of radiation effectiveness is expressed by RBE or QF.

Table 1. *Relationship between Linear Energy Transfer (LET) and Quality Factor (QF)*

LET∞		QF
MeV cm²/gm (H_2O)	(keV/μ in water)	
35 or less	3.5 or less	1
35–70	3.5–7.0	1–2
70–230	7.0–23	2–5
230–530	23–53	5–10
530–1750	53–175	10–20

LET∞ is the same as the "stopping power".

Curtis, Dye, and Sheldon[5] have approached the problem of radiation damage by considering the fractional number of cells of an organ killed, or inactivated, as a function of LET. They calculate a fractional cell lethality (FCL), using inactivation cross-sections shown in Fig. 3. Their results for the November 12, 1960 solar flare are shown as Figs. 4, 5, and 6, expressing the inactivation hits per cell per unit time-integrated particle flux. The abscissa value (P_0) is a measure of the momentum of the solar flare protons. Some of the inactivation cross-sections are those reported by Todd,[6] who determined the cross-sections for various types of tissue (including human kidney) under different conditions. His results are shown in Fig. 7, with the human kidney data shown in greater detail in Fig. 8. It is evident from these data that the high LET region is of great interest, in spite of the low flux of particles in space capable of producing these LET values.

It would also be desirable to measure the depth-dose distribution, since the dose generally exhibits a steep gradient with tissue depth. Figure 9 shows the depth-dose variation through the midline of an astronaut in the Apollo

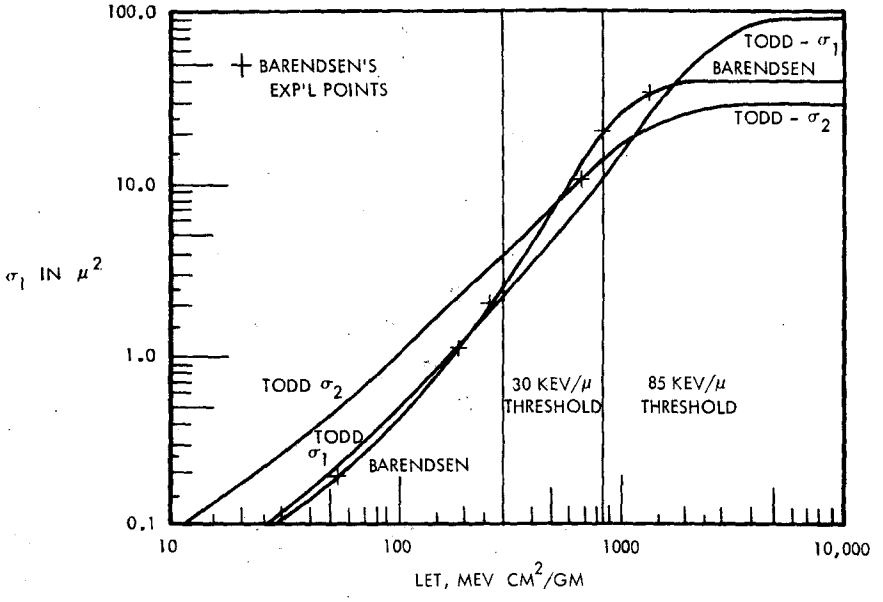

FIG. 3. Inactivation cross-sections.

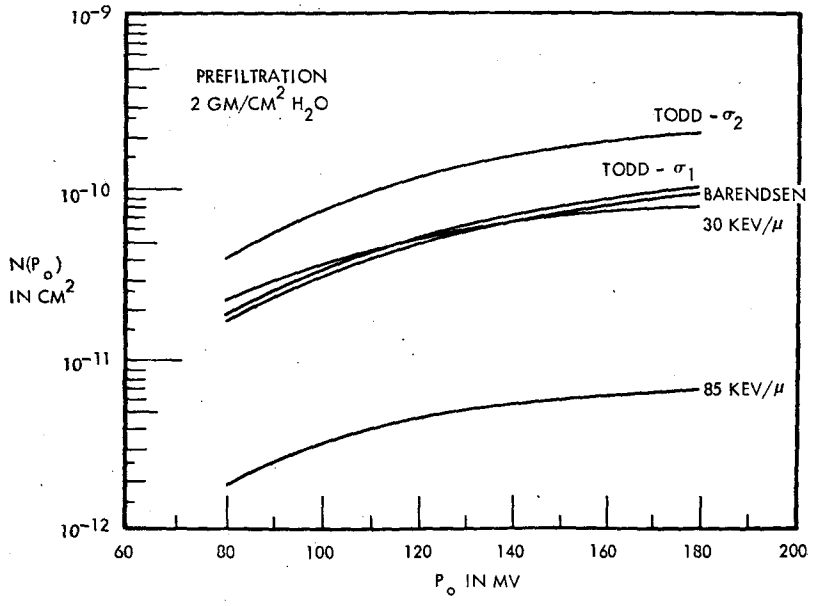

FIG. 4. Inactivation hits per cell per incident proton/cm^2.

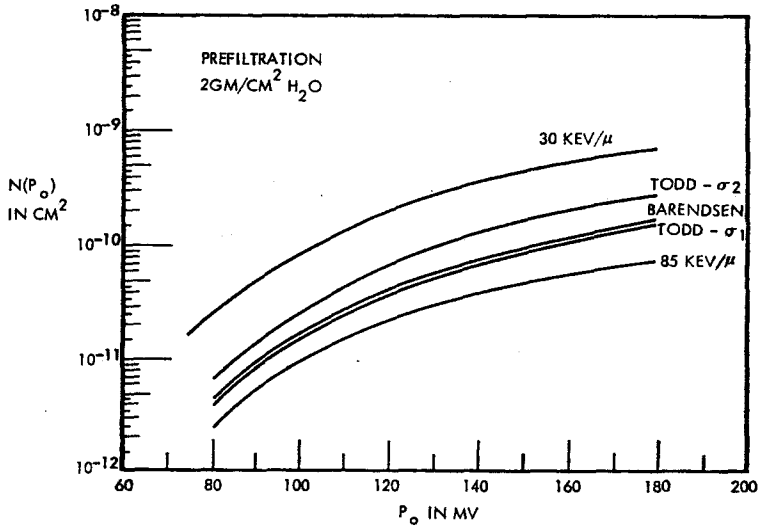

FIG. 5. Inactivation hits per cell per incident alpha/cm².

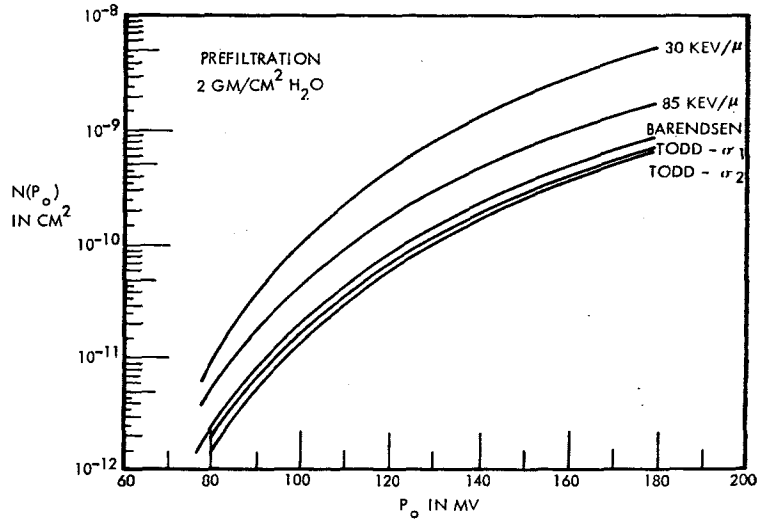

FIG. 6. Inactivation hits per cell per incident m-particle/cm².

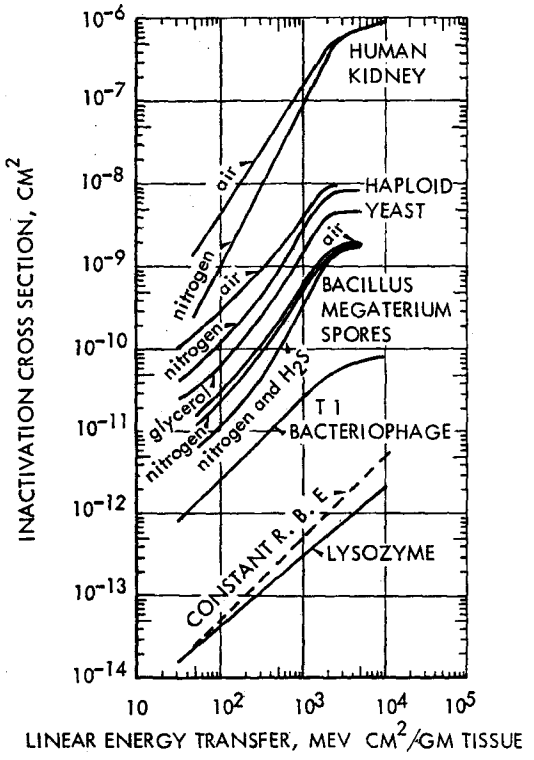

FIG. 7. Inactivation cross-sections of biological test objects obtained from experiments using the Berkeley HILAC

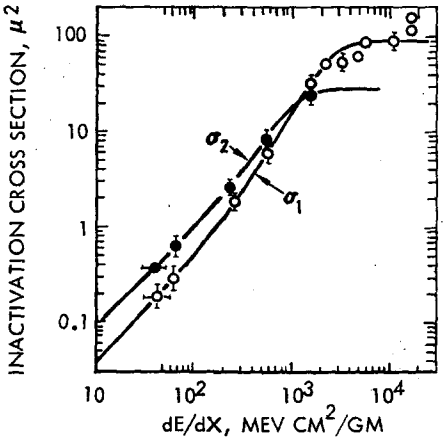

FIG. 8. Log-log plots of the inactivations cross-sections of human kidney (T1) cells *in vivo*; the probability of irreversible inactivation is expressed by σ_1, the initial slope of the "sigmoid" inactivation curves, and the probability of reversible inactivation (in which cells recover between fractionated doses) is expressed by σ_2, determined from the final slope of the inactivation curves.

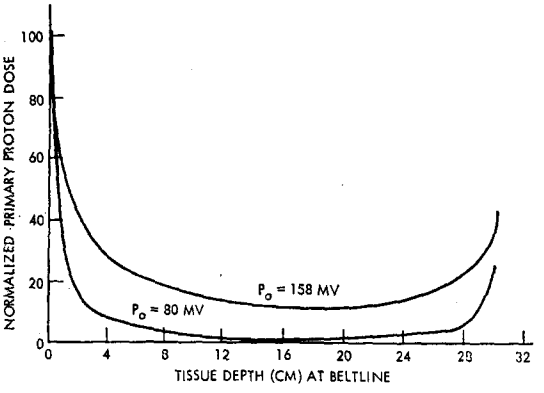

9. Depth dose variation for astronaut in Apollo command module.

command module, calculated for two solar flare spectra. It can be seen that, while a single depth point measurement is very valuable, a sampling of depth points would greatly enhance hazard evaluation.

To summarize, it is of great importance to determine the LET (absorbed dose distribution) spectra, total absorbed dose, and depth-dose distribution in space. To make a meaningful measurement, one must not introduce a detector so large that a dose gradient will exist within it. Present LET devices utilize large ion chambers which perturb the dose in the region being considered (in addition to many other defects of the ion chamber technique). It is felt that a much smaller device must be used, and be constructed of a tissue-like material, both in composition and density.

It is also desirable to know what percent of a population of cells are struck by the particles as they penetrate a tissue sample. Then, for these cells, one would like to know the distribution of energy losses in the cells. To complete the picture on a macroscopic scale, one would like the total absorbed dose rate and depth-dose distribution at several depths of tissue. These data then enable intelligent extensions to be made from laboratory experiments to conditions in space, and vice-versa.

SCIENTIFIC APPROACH

The concept of linear energy transfer (LET), although in use for some time, is difficult to place on a rigorous basis. LET refers to the energy transfer per unit length of the track of a charged particle traversing a medium. Since the energy deposition is a volume effect, this "linear" transfer is ambiguous; the transfer is certainly volume and geometry dependent. Limitations in this concept have recently been discussed by Rossi,[7] where he advocates use of a standard geometry (spherical), and reports distributions normalized to the diameter of the sphere. The proposed concept of a scintillator absorbed dose distribution (SADD) spectrometer is based on measurements of Rossi-type distributions in small spherical plastic scintillators the size of large cells.

The SADD system is a much improved technique for making absorbed dose distribution measurements. Its advantages over present ion-chamber systems are:

measurements with a detector the size of a cell

small size, resulting in negligible dose gradient through the detector

much better characteristics with regard to resolution and gain stability.

The reasons why scintillators have not been used previously are:

ion-chambers have been used extensively in radiobiological research in the past

widespread use of plastic scintillators has only recently occurred

new developments in photomultiplier tubes have resulted in much more precise and smaller systems than previously available

plastic scintillators exhibit different (non-linear) response for different types of particles (Fig. 10).

A close examination of the physics of the non-linear response of plastic scintillators to charged particles has resulted in a technique for solving the non-linear response problem for the SADD concept. It should be noted that the technique for folding in the path length distribution for the detector, a necessary method for interpreting data, is essentially the same as used in unfolding ion-chamber data.[8] It is believed that the SADD technique offers many advantages in absorbed dose distribution measurements over present systems.

As mentioned previously, devices presently used to measure LET are ion-chambers constructed of a "tissue-equivalent" wall, and filled with a "tissue-equivalent" gas. These detectors are large (2 in. dia.), and exhibit instability of gain and resolution. Consider now the new technique for LET measurement based on organic scintillation spectroscopy.

Organic scintillators have been used for some time. Of the many varieties, the plastic scintillator (a loaded polyvinyltoluene) has been chosen as being the best compromise for space use. Typical manufacturers are Nuclear Enterprises (NE-102) and Pilot Chemical (Pilot-B). The response of all organic scintillators to charged particles is quite similar, and varies according to particle type and energy. A typical response curve for an organic scintillator is shown as Fig. 10.[9]

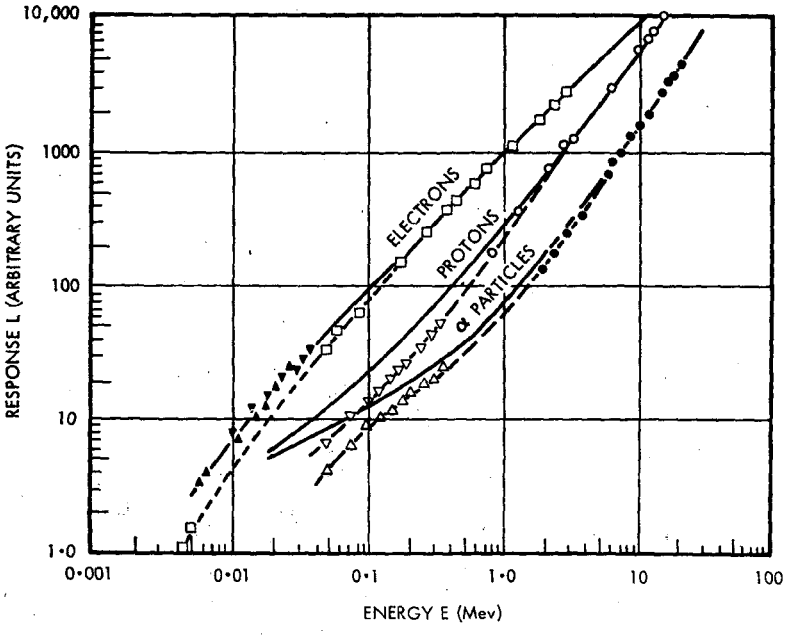

FIG. 10. Anthracene crystals: scintillation response to electronics, protons, and alpha particles (Brooks, 1956).

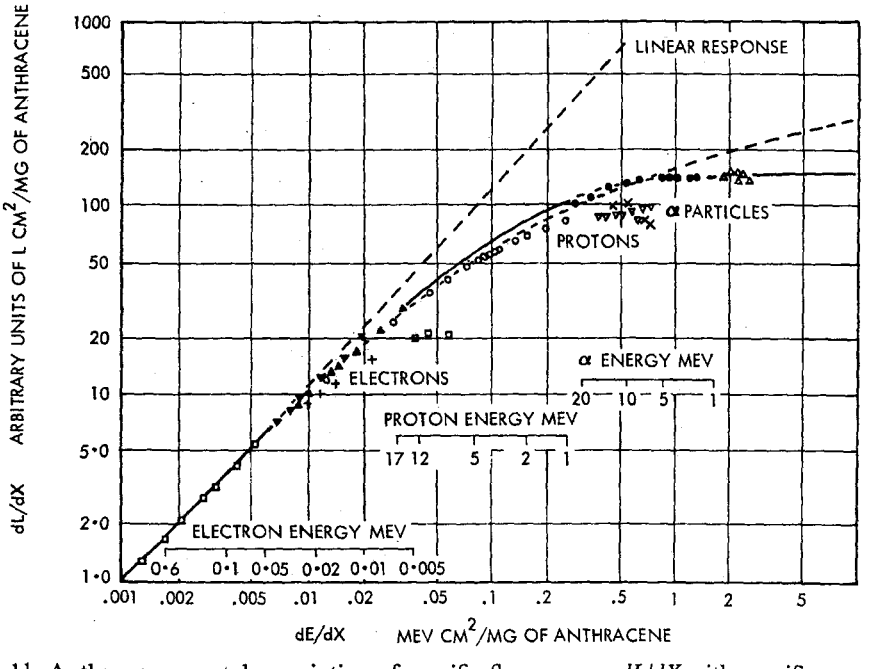

FIG. 11. Anthracene crystals: variation of specific fluorescence dL/dX with specific energy loss dE/dX (Brooks, 1956).

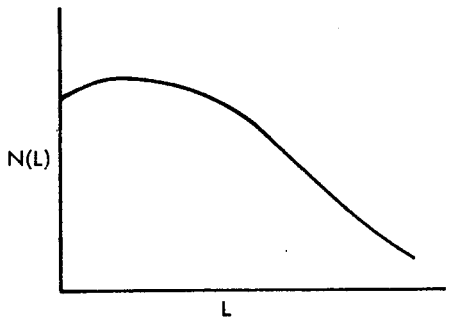

FIG. 12. Spectrum of particles incident on a plastic scintillator.

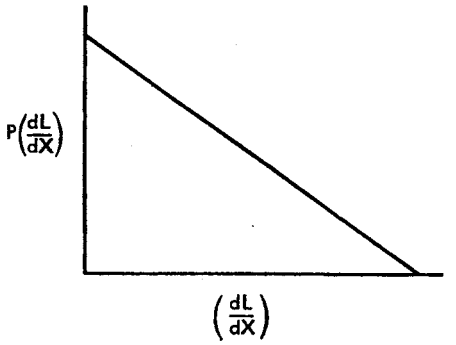

FIG. 14. Probability distribution of dL/dX.

However, if one considers the physics of this phenomenon, it is seen that the nonlinear response is related to the quenching of the primary excitation by the high local density of ionized and excited molecules. Birks[9] expresses this effect as

$$\frac{dL}{dX} = \frac{S\,(dE/dX)}{1 + k\,B(dE/dX)}$$

where L is light output, S is absolute scintillation efficiency, kB is a quenching constant, (dL/dX) is light output per unit path length, and (dE/dX) is energy loss per unit path length.

If one plots (dL/dX) vs. (dE/dX), a curve as shown in Fig. 11[9] is obtained. This result is very important, since the (dL/dX) spectrum is what the scintillator produces, and the spectrum of (dE/dX) is the desired end result. There is a one to one correspondence between $\frac{dL}{dX}$ and $\frac{dE}{dX}$ irrespective of the type of charged particle.

Suppose one measures, experimentally in space, the output spectrum for particles incident on a plastic scintillator, Fig. 12, where L is the light output from the scintillator. Assume also that the path length distribution in the detector is known, shown for a sphere in Fig. 13. Then, under the constraint that

$$L = \left(\frac{dL}{dX}\right) X \text{ or } \frac{dL}{dX} = \frac{L}{X},$$

i.e. dL/dX does not change appreciably in passing through the detector, one calculates, for each measured L point in the spectrum of $N(L)$ vs. L, the probability $P(L)$ that a given L was produced by a value of (dL/dX). The distributions for each L at specific values of (dL/dX) are summed and $N(L)$ vs. L has been transformed to $P\left(\frac{dL}{dX}\right)$ vs. (dL/dX), Fig. 14.

Using the relation of Birks between (dL/dX) and (dE/dX) as shown in Fig. 11, the probability

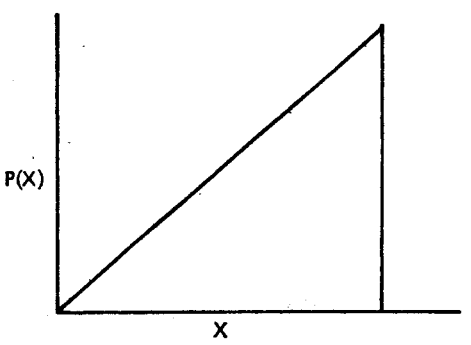

FIG. 13. Detector path length distribution.

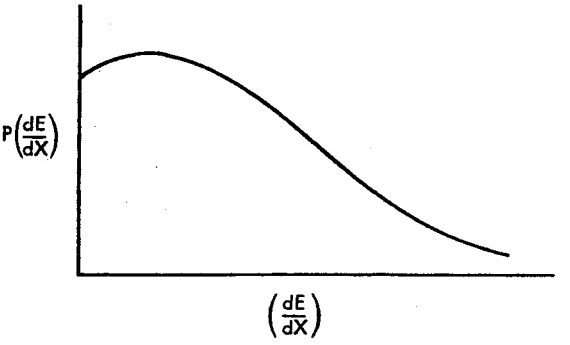

FIG. 15. Probability distribution of dE/dX.

distribution of (dE/dX) is calculated, Fig. 15. Note that by carrying the light output parameter (dL/dX) it is not necessary to know whether a particle producing the response is a proton, electron, or heavier particle. When transformation from (dL/dX) to (dE/dX) is made, again it is independent of the type of particle. Thus the problem of particle type-dependent response (e.g. Fig. 10) is removed.

Consider now the error introduced by particles stopped in the scintillator or in any detector (violation of the $L = \left(\frac{dL}{dX}\right) X$ assumption). If a particle is stopped one does not know and it is regarded as a lower dE/dX event than it actually is. Thus in the energy loss (dE/dX) spectrum, one shifts stopped particles from high to low LET, due to the self-shielding in the scintillator sphere.

The ambiguity in specifying dE/dX when a particle is stopped in the detector is reduced by making the detectors small. A 100 micron-path length (sphere diameter) stops approximately 2 meV protons and 80 keV electrons. Using the above method of converting the energy deposited to a (dE/dX), one would specify the particles to have had (dE/dX) of 20 keV/μ and 0.8 keV/μ respectively. The pulses generally fall in the low pulse-height channels (LOADD) and can be set aside for special data processing techniques. All other higher pulse heights must have been particles of high dE/dX passing through the detector, and fall into high pulse height channels (HIADD). There is a very small possibility of a galactic cosmic ray star event sending two or more highly ionizing particles through a sphere or spheres. This pulse would be counted as a single particle. Minimum ionizing particles ($dE/dX \approx 2$ meV cm^2/g) will leave approximately 20 keV pulse heights; these will be near, or below, the threshold of LOADD channel 1. Nominally, the threshold of LOADD channel 1 will be 40 keV (i.e. 0.4 keV/μ). The threshold perhaps could be lowered to 20 keV to include minimum ionizing particles, if it is deemed desirable. The sixteen channels will nominally be distributed from 0.4 keV/μ to $>$ 300 keV/μ (energy losses in the spheres from 4 meV cm^2/g to 3000 meV cm^2/g).

INSTRUMENTATION

Sensor Design

The sensor consists of spheres of NE 102 plastic scintillator surrounded by a specified depth of tissue equivalent material. The spheres approach the size of large cells, are approximately 100 microns or less in diameter, and are bonded to a lucite light pipe by an organic material such as solithane. The light pipe serves to couple the scintillators to the photomultiplier tube, and also provides a tissue-like backstop between the spheres and the quartz face of the photomultiplier tube, thus reducing the probability of back-scatter radiation from a non-tissue like material. Therefore, the scintillators experience an unperturbed dose field, closely approximating the ideal case of a tissue sample. There will be no appreciable air spaces or dissimilar materials near the detectors.

It is feasible to use spheres of 100 micron diameter or smaller. To obtain reasonable count rates for cosmic ray studies as well as for low energy–high flux background doses, it is necessary to expose a relatively large surface area to the ambient flux. This is accomplished by using many spheres, loosely spaced to reduce the probability of a single particle traversing more than one sphere. If one restricts the maximum count rate to 10^4 counts/sec, then approximately 1300 spheres would produce this rate in an omnidirectional flux of 10^5 particles/cm^2 sec. The same number of spheres would produce a count rate of 12.6 counts/min in a galactic cosmic ray flux of 2 particles/cm^2 sec.

The spheres, if closed-packed, would require being spread over an area of 0.02 in.^{2} (the area of a 0.14 in. dia. circle). Therefore it is feasible to achieve adequate loose spacing by using a 0.5 in. diameter circular base. This permits use of a small photomultiplier tube such as the ruggedized RCA 4460. A full-size sketch of the unit is shown as Fig. 16 for a tissue depth of 2 cm (no material pre-filtering).

A scintillator unit has been fabricated and is being used to examine the limitations of the technique. Sample NE-102 plastic spheres 100 +5/−9 microns have been obtained from Nuclear Enterprises, Ltd., of Canada, and the spheres have proved to be generally of uniform contour and free of bubbles. A uniform layer of spheres was cemented to a $\frac{1}{4}$ in. diameter by

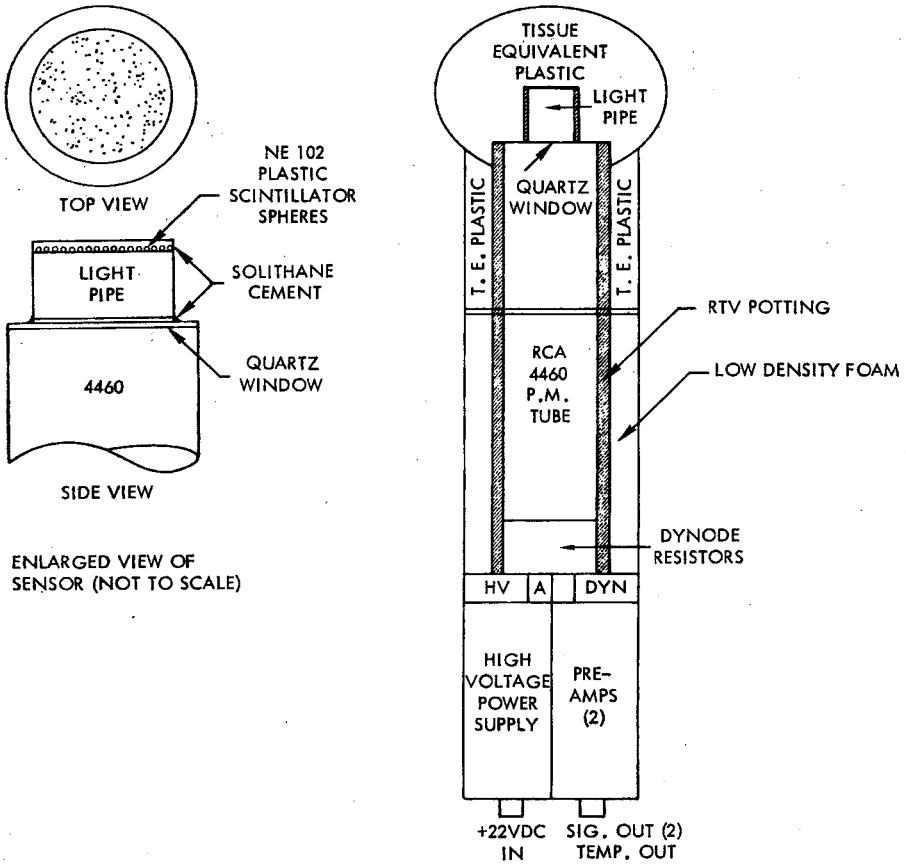

FIG. 16. Typical SADD sensor with 2 cm pre-filtering.

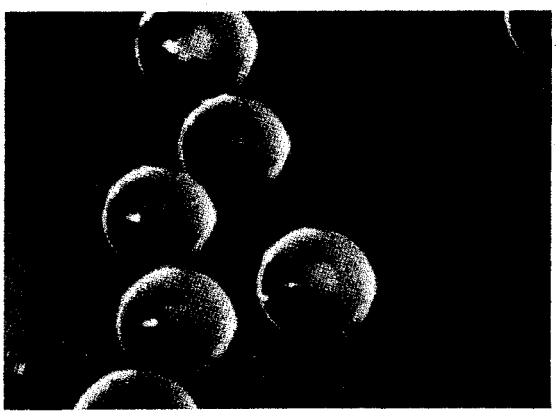

FIG. 17. 100 micron diameter spheres of NE-102 plastic scintillator.

$\frac{1}{4}$ in. thick lucite light pipe with a soft epoxy (solithane); Fig. 17 shows some of these spheres.

Two factors which limit the analysis of small pulses from the scintillators are the noise spectrums of the photomultiplier tube and self-scintillation of the lucite light pipe. These factors were investigated using an RCA 7767 photomultiplier tube (a typical tube not selected for low noise) and a lucite light pipe. The photomultiplier noise spectrum is shown in Fig. 18; no change was noted when the photomultiplier tube was irradiated with 0.1 millicurie of ^{137}Cs, or when the tube plus a $\frac{1}{2}$ in. diameter by $\frac{1}{2}$ in. thick piece of lucite were irradiated. The photomultiplier was then used with the lucite and the 100 micron spheres; the resulting pulse height spectrum is shown as Fig. 19. These tests indicate that analysis of

pulse heights down to 40 keV are certainly feasible; lower pulse heights may be analyzed if the system is optimized with respect to photomultiplier tube high voltage, temperature, selection for low noise, etc.

Signal Processing

The signals from the photomultiplier are processed by two preamplifiers, two eight channel differential pulse height analyzers, and two fifteen-bit binary storage registers. The dynamic range of each preamplifier-analyzer combination is approximately 30: 1. Thus, to accomplish analysis from 0.4 keV/μ to 300 keV/μ we propose to use two preamplifier analyzer combinations, one for low pulse heights (LOADD) and one for high pulse heights (HIADD) (it may be possible that no preamplifier is needed for the high pulse heights). If the preamplifier is connected in parallel, the low pulse height preamplifier must be nonoverloading at the high pulse heights. Each analyzer consists of a single channel analyzer, which shifts among eight attenuators to effectively yield eight channels of analysis. Note that the analysis proceeds sequentially in time, not simultaneously. The output is fed to a fifteen bit binary storage register. The sixteen channels of analysis will be distributed approximately logarithmically over the absorbed dose distribution range from 0.4 keV/μ to $>$ 300 keV/μ as Table 2.

A block diagram is shown as Fig. 20. Characteristics of one of the proposed preamplifiers and pulse height analyzers are shown as Fig. 21.[10]

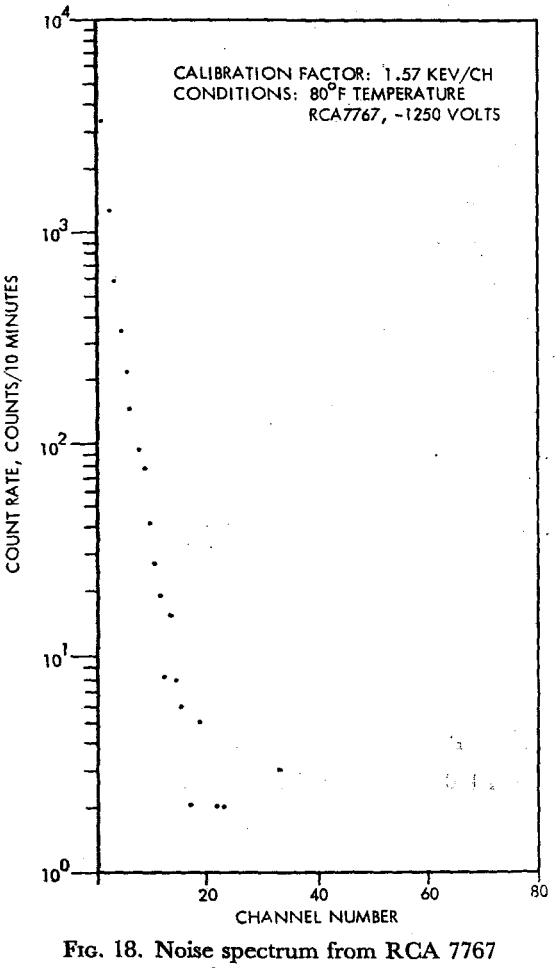

FIG. 18. Noise spectrum from RCA 7767 photomultiplier.

Table 2. Channel Distribution of Absorbed Doses

LOADD	HIADD
Channel 1: 0.4 < S < 0.6 keV/μ	12 < S < 20
Channel 2: 0.6 < S < 1.0 keV/μ	20 < S < 30
Channel 3: 1.0 < S < 2.0 keV/μ	30 < S < 50
Channel 4: 2.0 < S < 3.0 keV/μ	50 < S < 75
Channel 5: 3.0 < S < 5.0 keV/μ	75 < S < 100
Channel 6: 5.0 < S < 7.5 keV/μ	100 < S < 200
Channel 7: 7.5 < S < 10 keV/μ	200 < S < 300
Channel 8: 10 < S < 12 keV/μ	S > 300

The division of a pulse height spectrum into eight logarithmically distributed channels by the analyzer is shown in Fig. 21. This data was taken, not with a pulse generator, but with actual random pulses from a photomultiplier tube. The output from the flight pulse height analyzer was used to gate the same pulses into a 512 channel laboratory analyzer. This calibration technique allows one to determine exactly which pulses are counted in each flight analyzer channel with random pulses at various average counting rates. Some of the indicated variation in the threshold of the lowest channel is due to this calibration technique, which places pulses corresponding to this threshold in a very low channel number in the laboratory analyzer.

Data shown here were taken at an average

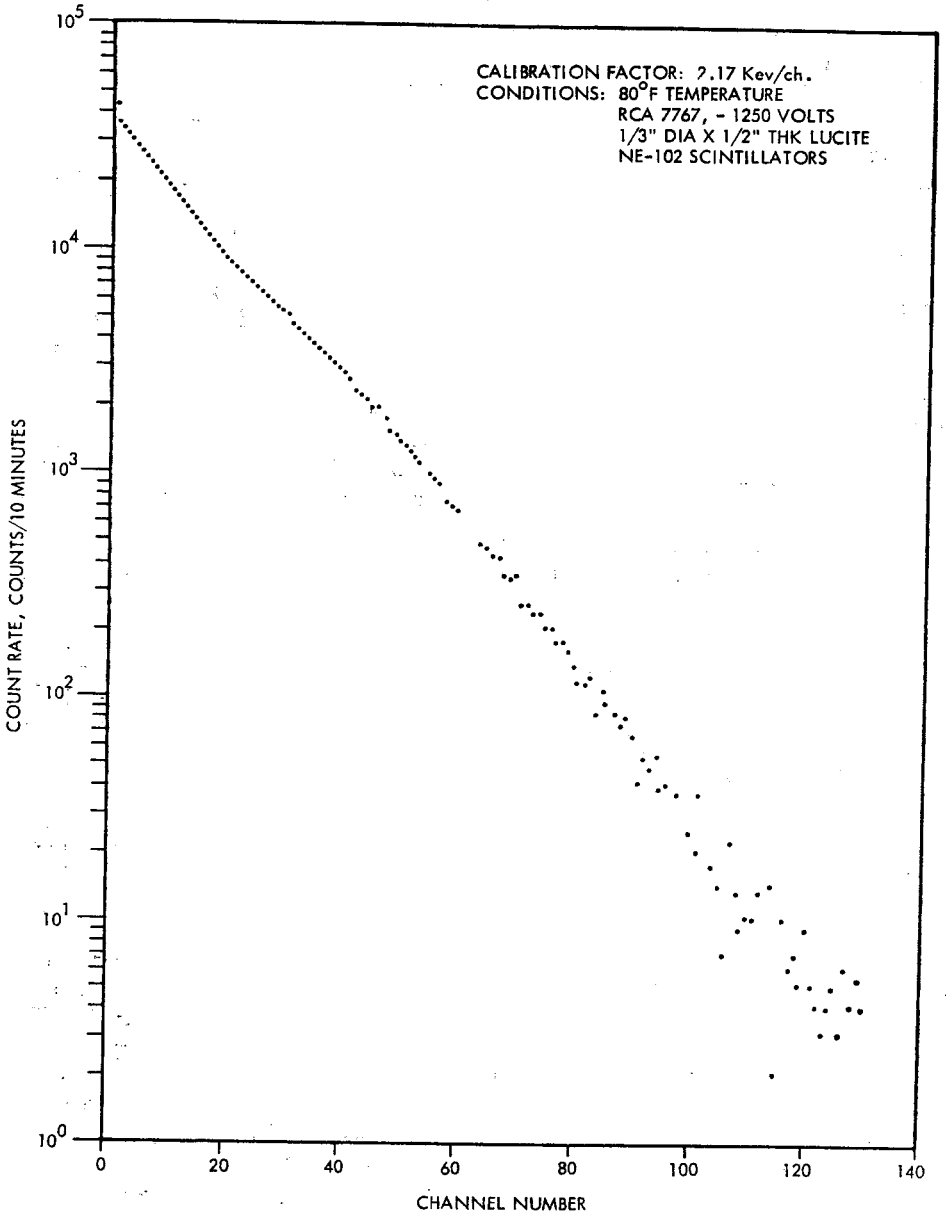

FIG. 19. Absorbed dose spectrum from 100 micron NE-102 spheres.

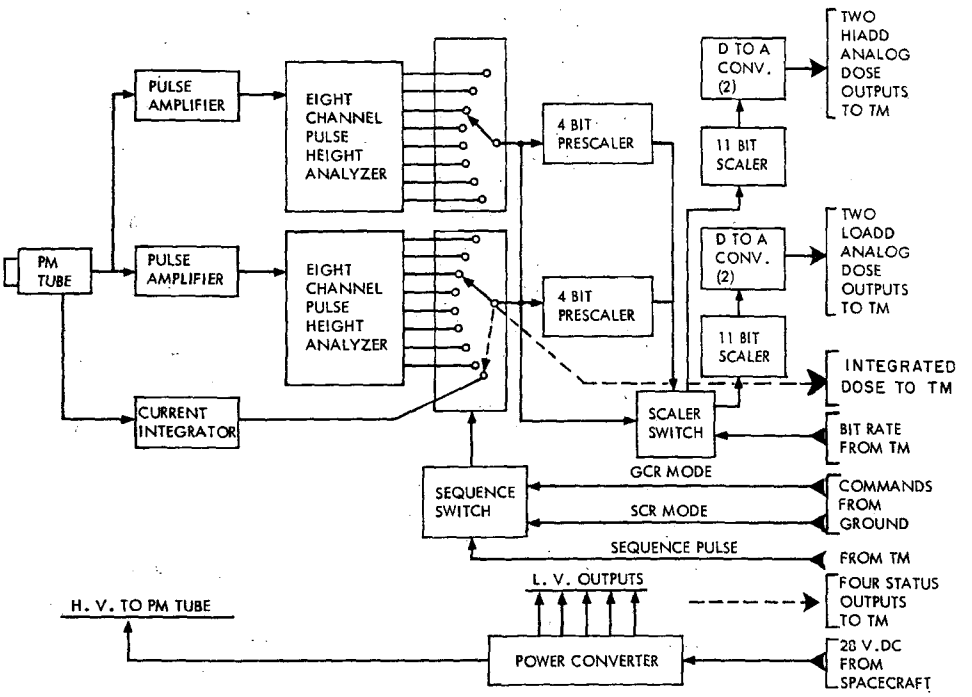

FIG. 20. Block diagram of electronics.

rate of 3000 pulses/sec. Significant shifts in the pulse height channels do not occur at rates up to 100,000 pulses/sec. Pulse pair resolution is about 400 nsecs. The temperature performance curves were taken with both the preamplifier and pulse height analyzer within the temperature chamber. Diagonal lines indicate gaps between channels, which occur at low temperatures. Some small overlap occurs at high temperatures, and is indicated by solid black areas. These gaps and overlaps are taken care of by calibration.

Each storage register contains an 8-bit D to A converter whose output is presented to the telemetry system. If PAM/FM telemetry is used, each storage register will feed two 6-bit D to A converters, and thus will require two data words on the commutator instead of one. The output from each channel will be sequentially read out. Note that for a PAM system the anode current (total absorbed dose) is not processed by the digital registers, but is presented directly to the telemetry in analog form from a readout circuit covering a dynamic range of four decades.

To operate satisfactorily in a quiet galactic cosmic ray (GCR) flux, a solar flare (SCR) event, or in a low energy, high-intensity electron background, different dose accumulation times will be used. In the low (GCR) mode, the registers will accumulate over 1 min, whereas in the high flux (SCR) mode, all channels will sum over 2 sec time periods. Normal operation will be 10 min in the GCR mode and 2 min in the SCR mode. Two ground commands are required to lock the instrument in either the SCR or GCR mode, to be used if one of the modes show marked superiority over the other.

The high voltage power supply produces regulated voltage for the photo-multiplier tube. The temperature dependence of the photomultiplier tube is compensated with a thermistor on the ninth dynode of the photomultiplier tube, which allows tube gain stabilization over a large temperature range. The low voltage power supply produces regulated voltages from an unregulated (28 V $\pm$ 5 V) input.

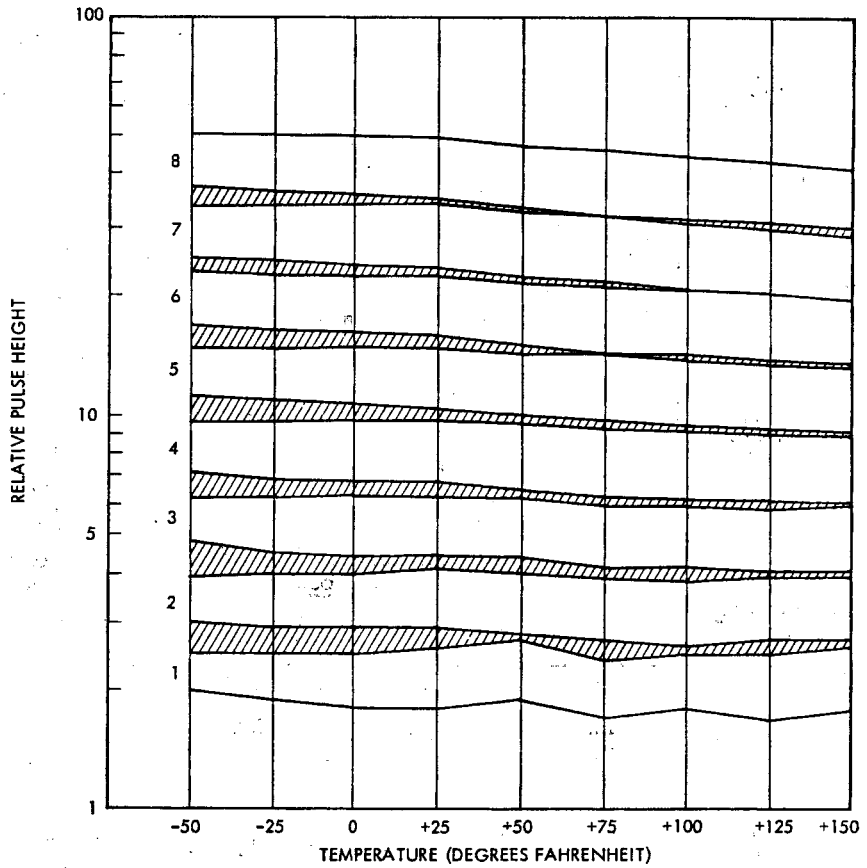

FIG. 21. Performance of preamplifier-pulse height analyzer combination.

Configuration

Design considerations divide the instrument into two packages. The first includes the photomultiplier assembly, high voltage power supply, and preamplifiers. The second package contains the remainder of the signal processing equipment, including the low voltage power supply. This flexible mounting arrangement enables the sensor to be placed in an optimum position for sampling the dose.

If the instrument is used on a manned spacecraft, the astronaut can change the tissue surrounding the detector, and thus obtain depth-dose measurements using one sensor. If the instrument is used on unmanned spacecraft, the depth-dose information is obtained by using several sensors with various amounts of tissue pre-filtering. The sensors can time-share the same electronics, or duplicate electronics can be used with attendant weight, power, volume, and telemetry penalties.

The technique is certainly applicable to ground-based laboratory use as well as for space flight measurements. The flexibility and sophistication of laboratory equipment permit much more precise measurements to be made.

Instrument specifications are detailed in Table 3.

CONCLUSION

The technique described in this paper makes possible a measurement of certain dosimetric parameters in a physically significant configuration. The actual detectors are of the density of tissue, and closely approximate the radiation-stopping powers of tissue. The size of the detectors approaches that of large cells (≤ 100

Table 3. Instrument Specifications

1. Power	2.0 W
2. Weight	4.0 lb
3. Volume	120 in^3 (electronics 4 × 5 × 5; sensor 1.5 × 1.5 × 7 in.)
4. Telemetry	Three analog words on main data commutator in SCR mode, i.e. three words read out at 2 sec intervals, and three words on subcommutator in GCR mode, i.e. three words read out at 1 min intervals. Four additional status words on subcommutator irrespective of mode. Note that PAM telemetry requires use of 6, 6, and 4 words.
5. Duty cycle	Continuous operation is desired, but reduced operation is acceptable.
6. Commands	4: ON, OFF, GCR mode, SCR mode.
7. Mounting requirements	To be determined.
8. Other desirable measurements	Trapped electrons and protons, solar flare protons and alpha particles, glactic cosmic rays, photons interior to vehicle, vehicle orientation, and vehicle location in position and time.
9. Temperature range	−50°F to +150°F survival operating; 0°F to +100°F

microns), and therefore measures energy depositions in a physically significant volume.

A pulse-height analysis of the signals from the sensor provides an absorbed dose distribution, while a measurement of the anode current from the photomultiplier tube is proportional to the total absorbed dose. Assignment of a weighting factor (such as a quality factor) to each channel of the absorbed dose distribution would lead to a direct readout of a biological dose, as compared with a physical dose (rads/hour). In addition, changing the tissue prefilter surrounding the 100 micron detectors can yield depth-dose distribution. Since the total number of spheres is known, and each pulse represents a bit of one sphere, information on the cell hit frequency is directly obtainable.

The technique can be applied using many instrument configurations. The limitations of the concept are currently being investigated both in the laboratory and in space; the first space flight of an instrument using this technique is scheduled for spring of 1967. It is believed by the authors that this technique has many advantages over present ion-chamber techniques, the more important being the physical characteristics of the dosimeters and the calibration stability of the instrument.

REFERENCES

1. H. J. Schaefer. Local dose from proton and alpha particle enders behind complex shield systems. *Proc. Second Symposium on Protection against Radiation in Space*, Gatlinburg, Tennessee, 1964.
2. National Bureau of Standards. U.S. Department of Commerce. Report of the International Commission on Radiological Units and Measurements (ICRU) 1959, Handbook No. 78, U.S. Government Printing Office, Washington, D.C., 1961.
3. J. W. Haffner. RBE of protons and alpha particles. *Proc. Second Symposium on Protection against Radiation in Space*, Gatlinburg, Tennessee, 1964.
4. R. Madey and T. E. Stephenson. Quality factors for degraded proton spectra, Ibid.
5. S. B. Curtis, D. L. Dye and W. R. Sheldon. Fractional cell lethality approach to space radiation hazards.
6. P. Todd. Biological effects of heavy ions. Ibid.
7. H. H. Rossi. Specification of radiation quality. *Rad. Res.* **10,** 522 (1959).
8. H. H. Rossi and M. S. Rosenzweig. A device for the measurement of dose as a function of specific ionization. *Radiology* **64,** 404 (1955).
9. J. B. Birks. *The Theory and Practice of Scintillation Counting*, Pergamon Press, New York, 1964.
10. T. A. Farley. Institute of Geophysics, University of California at Los Angeles, private communication, 1965.